Neurotherapeutics (2019) 16:1255–1268
https://doi.org/10.1007/s13311-019-00770-z

ORIGINAL ARTICLE

Cyclooxygenase-2 Induced the β-Amyloid Protein Deposition and Neuronal Apoptosis Via Upregulating the Synthesis of Prostaglandin E_2 and 15-Deoxy-$\Delta^{12,14}$-prostaglandin J_2

Pei-Pei Guan[1] · Yun-Yue Liang[1] · Long-Long Cao[1] · Xin Yu[1] · Pu Wang[1]

Published online: 7 August 2019

Abstract

Elevated levels of cyclooxygenase-2 (COX-2) and prostaglandins (PGs) have been shown to be involved in the pathogenesis of Alzheimer's disease. Analysis of the underlying mechanisms elucidated a function of sequential PGE_2 and PGD_2 synthesis in regulating β-amyloid protein (Aβ) deposition by modulating tumor necrosis factor α (TNF-α)-dependent presenilin (PS)1/2 activity in COX-2 and APP/PS1 crossed mice. Specifically, COX-2 overexpression accelerates the expression of microsomal PGE synthase-1 (mPGES-1) and lipocalin-type prostaglandin D synthase (L-PGDS), leading to the synthesis of PGE_2 and 15-deoxy-$\Delta^{12,14}$-prostaglandin J_2 (15d-PGJ_2) in 6-month-old APP/PS1 mice. Consequently, PGE_2 has the ability to increase Aβ production by enhancing the expression of PS1/2 in a TNF-α-dependent manner, which accelerates the cognitive decline of COX-2/APP/PS1 mice. More interestingly, low concentrations of 15d-PGJ_2 treatment facilitate the effects of PGE_2 on the deposition of Aβ via TNF-α-dependent PS1/2 mechanisms. In contrast, high concentrations of 15d-PGJ_2 treatment inhibit the deposition of Aβ via suppressing the expression of TNF-α-dependent PS1/2. In this regard, a high concentration of 15d-PGJ_2 appears to be a therapeutic agent against Alzheimer's disease. However, the high 15d-PGJ_2 concentration treatment induces neuronal apoptosis via increasing the protein levels of Bax, cleaved caspase-3, and DFF45, which further impairs the learning ability of APP/PS1 mice.

Key Words COX-2 · PGE_2 · 15d-PGJ_2 · TNF-α · presenilin1/2 · apoptosis.

Abbreviations

COX-2	Cyclooxygenase-2
PGs	Prostaglandins
AD	Alzheimer's disease
Aβ	β-Amyloid protein
TNF-α	Tumor necrosis factor α
PS	Presenilin
mPGES-1	Microsomal PGE synthase-1
15d-PGJ_2	15-Deoxy-$\Delta^{12,14}$-prostaglandin J_2
L-PGDS	Lipocalin-type prostaglandin D synthase
NSAIDs	Nonsteroidal anti-inflammatory drugs
APP	β-Amyloid precursor protein
APs	β-Amyloid plaques

Electronic supplementary material The online version of this article (https://doi.org/10.1007/s13311-019-00770-z) contains supplementary material, which is available to authorized users.

✉ Pu Wang
wangpu@mail.neu.edu.cn

[1] College of Life and Health Sciences, Northeastern University, No. 3-11, Wenhua Road, Shenyang 110819, China

Introduction

Alzheimer's disease (AD) is the most common form of dementia in people over 65 years of age and is characterized clinically by cognitive decline and pathologically by the accumulation of β-amyloid protein (Aβ) and hyperphosphorylation of tau in the brain. Although there is no cure for this fatal disease, recent evidence has shown that overexpression of cyclooxygenase-2 (COX-2) has the ability to induce cognitive decline of APP/PS1 Tg mice [1–3], most likely due to the accumulation of Aβ in neurons [4]. By inhibiting the activity of COX-2, flurbiprofen improves the learning ability of Tg2576 mice [5]. More closely, long-term treatment with celecoxib, a selective COX-2 inhibitor, alleviates the brain Aβ load by 22% in APP/PS1 mice [6]. Apart from COX-2, knocking out the expression of mPGES-1, a

PGE_2 synthase, exerts positive effects on ameliorating the aggregation of Aβ in β-amyloid plaques (Aps) [7]. Moreover, PGE_2, the metabolic product of mPGES-1, mediated the effects of IL-1β on impairing the learning abilities of Wistar and Sprague-Dawley rats [8, 9]. More interestingly, EP2–4 are PGE_2 receptors involved in mediating the effects of Aβ on Aβ accumulation in the brains of APP23 mice [10, 11]. In contrast, the roles of L-PGDS and its metabolic products, including PGD_2 and 15-deoxy-$\Delta^{12,14}$-prostaglandin J2 (15d-PGJ_2), in the pathogenesis of AD are not fully elucidated. In patients with DESH, high levels of L-PGDS exert stimulatory effects on the phosphorylation of tau, which impairs the learning ability of patients [12]. In line with this observation, L-PGDS has been shown to induce cognitive decline by forming APs in the brains of AD patients and Tg2576 mice [13]. Unfortunately, these observations have not been extended to PGD_2 and 15d-PGJ_2, and the underlying mechanisms are highly overlooked.

Although the mechanisms of COX-2 in AD are not fully elucidated, the role of COX-2 in exacerbating AD cannot be negated. For example, inhibition by prolonged treatment with nonsteroidal anti-inflammatory drugs (NSAIDs) has been shown to delay or prevent the onset of AD in clinical trials [14]. In agreement with these results, celecoxib, a COX-2-specific inhibitor, has shown the ability to decrease the Aβ load in the brains of APP/PS1 Tg mice [1, 6]. Regarding other NSAIDs, ibuprofen, a COX-2 nonspecific inhibitor, has also been shown to decrease the levels of Aβ in Tg2576, 3XTg, and APPV7171 mice [15–19]. R-flurbiprofen and triflusal also showed inhibitory effects on the production of Ab in Tg2576 mice [5, 20].

Given the potential role of COX-2 in AD progression, COX-2 usually exacerbates AD via upregulating the expression of proinflammatory cytokines as an important proinflammatory factor. For instance, PGE_2 treatment increases the expression of tumor necrosis factor α (TNF-α) in SH-SY5Y cells [21]. In addition, lipocalin-type prostaglandin D synthase (L-PGDS) upregulation is responsible for the synthesis of TNF-α in AD patients [22]. In contrast, 15d-PGJ_2 treatment attenuates the expression of TNF-α in primary cultured astrocytes and microglial cells [23, 24]. As the downstream target of COX-2, TNF-α upregulation is also involved in accelerating the development of AD. Specifically, TNF-α upregulates APP processing and Aβ deposition in human rhabdomyosarcoma [25] and neuroblastoma cells [26]. In addition, anti-TNF-α or the inhibition of TNF-α signaling reduces the formation of APs in the brains of APP/PS1 transgenic mice [27, 28]. These excerpted reports thereby indicate a possible role of COX-2 in exacerbating AD via TNF-α.

However, TNF-α cannot exert its effects in a vacuum to affect the development and progression of AD. Indeed, TNF-α has been shown to promote the cleavage of β-amyloid precursor protein (APP). For example, TNF-α can induce the activity of BACE-1, which results in the β-cleavage of APP in $APP^{+/-}$/$GRKO^{-/-}$ mice [29–31]. In addition, TNF-α is also responsible for the γ-cleavage of APP by activating PS1 and PS2 in HEK293 and SK-N-SH cells [32, 33]. By these potential mechanisms, TNF-α might be responsible for mediating the effects of COX-2 and PGs on regulating the production of Aβ.

As discussed above, L-PGDS was shown to induce cognitive decline by forming APs in the brains of AD patients and Tg2576 mice [13], and the metabolic product of L-PGDS could also feasibly be involved in the development and progression of AD. For example, 15d-PGJ_2, a metabolic product of L-PGDS, has been reported to inhibit the production of cytokines, such as TNF-α, IL-1β, IL-6, NO, MCP-1 and IL-12, in astrocytes and microglial cells, which are responsible for the pathogenesis of AD [23, 24, 34, 35]. More interestingly, PGD_2 has the ability to induce apoptosis in primary cultured rat microglial cells [36]. In addition, 15d-PGJ_2, a dehydrated product of PGD_2, has the ability to induce the production of Z-VAD in primary cultured rat cortical neurons and SH-SY5Y cells [37].

In these previous studies, multiple *in vivo* AD experimental models were utilized. Using sophisticated molecular techniques, we explored the intracellular mechanisms by which COX-2 induces the production of TNF-α- and presenilin (PS)1/2-dependent Aβ deposition via PGE_2 and 15d-PGJ_2.

Experimental Procedures

Reagents

NS398, PGE_2, and 15d-PGJ_2 and antibodies specific for mPGES-1 and L-PGDS were obtained from Sigma-Aldrich Corp. (St. Louis, MO, USA). Antibodies against β-actin (#4970, 1:5000, v/v), COX-2 (#12282, 1:2000, v/v), TNF-α (#3707, 1:2000, v/v), PS1 (#5643, 1:2000, v/v), PS2 (#2192, 1:2000, v/v), and Aβ (#2450, 1:500, v/v) were purchased from Cell Signaling Technology, Inc. (Danvers, MA, USA). PGE_2, 15d-PGJ_2, and TNF-α enzyme-linked immunosorbent assay kits were purchased from Cayman Chemical (Ann Arbor, MI, USA), Assay Designs (Ann Arbor, MI, USA), Invitrogen (Carlsbad, CA, USA), and RayBiotech, Inc. (Norcross, GA, USA), respectively. All reagents for the qRT-PCR and SDS-PAGE experiments were purchased from Bio-Rad Laboratories (Shanghai, China). All other reagents were purchased from Sigma-Aldrich Corp. (St. Louis, MO, USA) unless otherwise specified.

Cell Culture and Treatment

Mouse neuroblastoma 2a (N2a) cells were grown (37 °C and 5% CO_2) on 6-cm tissue culture dishes (10^6 cells per dish) in

appropriate medium. In a separate set of experiments, the cells were grown in serum-free medium for an additional 12 h before incubation with the indicated concentrations of 15d-PGJ_2 (0, 10, 20, 50, 100, 200, or 500 nM) for 24 h. The medium and/or cells were then collected and lysed for the analysis of ELISA and Western blots.

Transgenic Mice

Female wild-type (WT), APP/PS1 transgenic [B6C3-Tg (APPswe, PSEN1dE9) 85Dbo/J (stock number 004462)] (Tg), and COX-2 transgenic [C57BL/6J-Tg(Thy1-PTGS2)303Kand/J (stock number 010703)] mice were obtained from Jackson Laboratory (Bar Harbor, ME, USA). Of note, the PGE_2 levels in COX-2 transgenic mice are ~25- to 40-fold greater than those in nontransgenic controls based on information provided by Jackson Laboratory. Genotyping was performed 3 to 4 weeks after birth. Mice were housed at 6 per cage in a controlled environment at standard room temperature and relative humidity on a 12-h light–dark cycle and had free access to food and water. To generate mice heterozygous for both the COX-2 and APP/PS1 transgenes, COX-2 males were bred with APP/PS1 females. In select experiments, mice at the age of 3 months were intranasally administered PGE_2 (2 μg/20 μl/day) or 15d-PGJ_2 (20 or 1000 ng/20 μl/day) for 3 months before their learning ability was assessed by the Morris water maze test or the nest construction assay. In select experiments, the mice were injected (intracerebroventricularly, i.c.v.) with the indicated concentrations of PGE_2, 15d-PGJ_2, or NS398 (1 μg/5 μl) for 24 h before measuring the expression of mPGES-1, L-PGDS, TNF-α, PS1, or PS2.

Morris Water Maze

The mice were trained and tested in a Morris water maze as previously described [38]. In brief, the mice were pretrained in a circular water maze with a visible platform for 2 days. The platform was then submerged inside the maze, with the deck 0.5 cm below the surface of the water for the following experiments. Milk was added to the water to hide the platform from sight. The mice were placed inside the maze to swim freely until they found the hidden platform. The entire experiment lasted for 7 days. For the first 6 days, the mice were left in the maze for a maximum time of 60 s and allowed to find the platform. The learning sessions were repeated for 4 trials each day, with an interval of 1 h between each session. The spatial learning scores (the latency period necessary to find and climb onto the hidden platform and the length of the path to the platform) were recorded. On the last day, the platform was removed, and the number of times that the mice passed through the memorized region was recorded for a period of 2 min (120 s). Finally, the recorded data were analyzed statistically with a computer program (ZH0065; Zhenghua Bioequipment, Yuanyang City, Henan, China).

Nest Construction

Nest construction was tested and analyzed as previously described [38]. In brief, the mice were housed in corncob bedding for 1 week before the nest construction test. Two hours before the onset of the dark phase of the light cycle, 8 pieces of paper (5 × 5 cm^2) were introduced into the home cage to create conditions for nesting. The nests were scored the following morning according to a 4-point system: 1, no biting/tearing of paper, with random dispersion of the paper; 2, no biting/tearing of paper, with gathering of the papers in a corner/side of the cage; 3, moderate biting/tearing of paper, with gathering of the papers in a corner/side of the cage; and 4, extensive biting/tearing of paper, with gathering of the papers in a corner/side of the cage.

Cerebrospinal Fluid Collection

CSF was collected as previously described [38–41]. In brief, the mice were anesthetized and placed prone on the stereotaxic instrument. A sagittal incision of the skin was made inferior to the occiput. Under the dissection microscope, the subcutaneous tissue and neck muscles through the midline were bluntly separated. A microretractor was used to hold the muscles apart. Next, the mouse was positioned such that the body made a 135° angle with the fixed head. At this angle, the dura and spinal medulla were visible and had a characteristic glistening and clear appearance, and the circulatory pulsation of the medulla (i.e., a blood vessel) and adjacent CSF space could be seen. The dura was then penetrated with a 6-cm-long glass capillary that had a tapered tip with an outer diameter of 0.5 mm. Following a noticeable change in resistance to the capillary insertion, the CSF flowed into the capillary. The average volume of CSF obtained was approximately 7 μl. All samples were stored in polypropylene tubes at − 80 °C until the concentrations of PGE_2, 15d-PGJ_2, and TNF-α were measured.

Stereotaxic Injection

NS398 (1 μg/5 μl) or vehicle (PBS) was injected (i.c.v.) into COX-2/APP/PS1 mice as previously described [42]. In brief, stereotaxic injectors were placed at the following coordinates relative to bregma: mediolateral, 21.0 mm; anteroposterior, 20.22 mm; and dorsoventral, 22.8 mm. Twenty-four hours after injection, the mice were anesthetized and subjected to perfusion as previously described [38, 41].

Immunohistochemistry

Brain tissues were collected from the mice. Serial sections (10 μm thick) were cut by cryostat (Leica, CM1850, Germany). The slides were rehydrated in a graded series of ethanol and submerged in 3% hydrogen peroxide to eliminate endogenous peroxidase activity. The levels of COX-2, PS1, PS2, and Aβ were determined with an immunohistochemical staining kit, according to the manufacturer's instructions (Life Technologies/Invitrogen). In brief, frozen sections of mouse brain were treated with 5% bovine serum albumin for 1 h and then incubated with either rabbit anti-COX-2, PS1/2, or Aβ (1:500, Cell Signaling Technology) overnight at 4 °C. After washing, the sections were incubated with biotinylated IgG (1:200) for 1 h at room temperature, followed by incubation with streptavidin peroxidase for 30 min. After thorough rinsing, the sections were treated with 0.025% 3,3-diaminobenzidine plus 0.0033% H_2O_2 in TBS for 5 min. The stained sections were dehydrated, cleared, and mounted with neutral balsam. The sections were examined, and images were obtained with a Leica microscope.

Immunofluorescence

Brain tissues were collected from APP/PS1 transgenic mice. Serial sections (10 μm thick) were cut using a cryostat (Leica, CM1850, Germany). The slides were rehydrated in a graded series of ethanol and submerged in 3% hydrogen peroxide to eliminate endogenous peroxidase activity. Colocalization of COX-2 with Aβ and microglial cells was determined with an immunofluorescence staining kit according to the manufacturer's instructions (MXB Biotechnologies, Fuzhou, China). In brief, frozen sections of mouse brain were treated with 5% bovine serum albumin for 1 h and then incubated with either rabbit anti-COX-2 (1:500, Cell Signaling Technology) or PS1/2 (1:500, Cell Signaling Technology) together with mouse Aβ (1:500, #A8354, Sigma-Aldrich Corp., St. Louis, MO, USA), Iba-1 (1:500, #GT10312, Thermo Fischer Scientific, Shanghai, China), or NeuN (1:500, #ab104224, Abcam, Shanghai, China) overnight at 4 °C. After washing, the sections were incubated with Alexa Fluor 555 or 488 secondary antibodies (1:200, Cell Signaling Technology) for 1 h at room temperature. After thorough rinsing, the stained sections were dehydrated, cleared, and mounted with a fluorescent sealing agent. The sections were examined, and images were obtained with a Leica microscope.

Western Blot Analysis

Tissues or cells were washed with PBS (−) and lysed in 500 μl of RIPA buffer containing protease inhibitor cocktail (Pierce Chemical Company). The protein contents in the cell lysates were determined using a bicinchoninic acid protein assay reagent (Pierce Chemical Company, Shanghai, China). The protein samples were mixed with loading buffer and boiled for 5 min at 100 °C. Aliquots of total cell lysates were subjected to SDS-PAGE, transferred onto a nitrocellulose membrane, and probed with a panel of specific antibodies. Each membrane was probed using only 1 antibody. β-Actin was used as a loading control. All Western hybridizations were performed at least in triplicate, and a different cell preparation was used each time.

qRT-PCR

qRT-PCR assays were performed with the MiniOpticon Real-Time PCR detection system (Bio-Rad Laboratories) using total RNA and the GoTaq One-step Real-Time PCR kit with SYBR green (Promega, Madison, WI). Forward and reverse primers for mouse PS2 were 5′-CACTCTTCCTGGCT GTCTGG-3′ and 5′-CCACACCATGGCAGATGAGT-3′, respectively. The gene expression levels were normalized to GAPDH, whose forward and reverse primers were 5′-GCTC ATGACCACAGTCCATGCCAT-3′ and 5′-TACT TGGCAGGTTTCTCCAGGCGG-3′, respectively.

Measurement of PGE_2, 15d-PGJ_2, and TNF-α Concentrations

The PGE_2, 15d-PGJ_2, and TNF-α levels in the CSF of both control and pharmacologically treated mice were determined using PGE_2, 15d-PGJ_2, and TNF-α enzyme immunoassay kits according to the manufacturer's instructions. In brief, an IgG antibody was precoated onto 96-well plates. Standards or test samples were added to the wells together with an alkaline phosphatase (AP)-conjugated PGE_2, 15d-PGJ_2, or TNF-α antibody. After incubation, the excess reagents were washed away, and a pNpp substrate was added and catalyzed by AP to produce a yellow color. The intensity of the yellow coloration was inversely proportional to the amount of PGE_2, 15d-PGJ_2, or TNF-α captured on the plate.

Brain Tissue Extracts

The brains were removed and isolated from the mice as previously described unless stated otherwise [38, 41]. Tissues were then homogenized in RIPA buffer, vortexed, sonicated for 3.5 s, and centrifuged at 3000×*g* for 5 min. The supernatant was then aliquoted and frozen.

Animal Committee

All animals were handled according to the Guide for the Care and Use of Medical Laboratory Animals (Ministry of Health, People's Republic of China, 1998), and all experimental

protocols were approved by the Laboratory Ethics Committees of China Medical University and the College of Life and Health Sciences of Northeastern University.

Statistical Analysis

For each *in vivo* study, approximately 6 mice per group were studied. All data are represented as the mean ± S.E. Differences among means were analyzed using analysis of variance (ANOVA). The Newman–Keuls post hoc test was used to assess pairwise comparisons between means. Differences between means were analyzed using a 2-tailed Student's *t* test [39]. In all analyses, the null hypothesis was rejected at the 0.05 level. The statistical analyses were performed using the Prism Stat program (GraphPad Software, Inc., San Diego, CA, USA).

Results

COX-2 Expression Is Elevated at the Early Stage of AD and Deposited in Amyloid Plaques at the Late Stage of AD

Consistent with previous findings [43, 44], COX-2 expression was upregulated in early AD patients and 3- to 6-month-old APP/PS1 mice (Fig. 1A). Interestingly, the markedly induced COX-2 tended to return toward basal levels in 18-month-old APP/PS1 mice (Fig. 1A). Moreover, morphological observations showed that COX-2 immunostaining was highly induced in the brains of 3- or 6-month-old APP/PS1 mice (Fig. 1B). Interestingly, morphological observations showed that COX-2 immunostaining was similar to that of Aβ (Fig. 1B), which indicates the possible heteroaggregation of COX-2 and Aβ in 18-month-old APP/PS1 mice. In line with our observations, Nagano et al. [45] reported that COX-2 cross-linked with Aβ, which potentially inhibits Aβ metabolism and generates toxic intracellular forms of oligomeric Aβ. We therefore assessed the colocalization between COX-2 and Aβ. By double-staining, COX-2 clearly resided in the APs (Fig. 1C). As an important inducer of inflammation, we further determined the relationship between COX-2 and microglial cells, demonstrating that COX-2 colocalized with microglial cells (Fig. 1D). Collectively, these findings suggest that early induced COX-2 may contribute to Aβ deposition in APs during the course of AD development and progression.

COX-2 Overexpression Exacerbates the Cognitive Decline of APP/PS1 Mice

We next investigated the relationship between brain COX-2 activity and learning ability in APP/PS1 mice. To this end, we bred male COX-2 mice with female APP/PS1 mice. We used these 6-month-old COX-2/APP/PS1 mice for Morris water maze and nest construction experiments. The results demonstrated that COX-2 overexpression exacerbated the cognitive decline of 6-month-old APP/PS1 mice (Fig. 2A–F). Thus, these results support the fact that COX-2 exacerbates cognitive decline during the course of AD development.

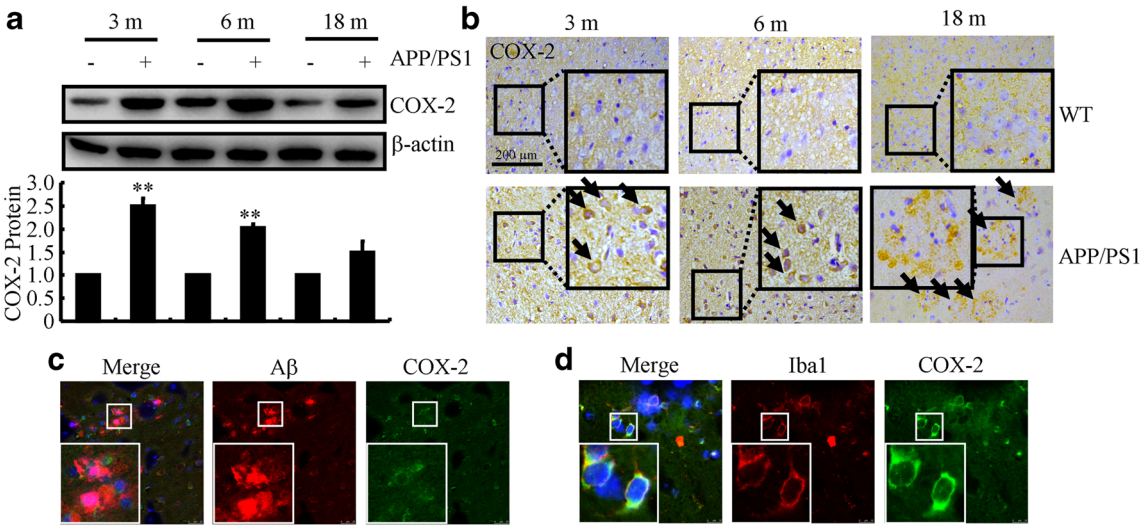

Fig. 1 COX-2 expression is upregulated at the early stage of AD, and then aggregates around APs at the late stage of AD. APP/PS1 Tg mice at different ages were collected ($n = 6$). (A) Total protein was extracted by RIPA buffer. The COX-2 protein level was determined by Western blots. β-Actin served as an internal control. (B) The brains of APP/PS1 mice were sliced by cryostat (10 μm), and the immunoreactivity of COX-2 was determined by immunohistochemistry. The cerebral cortex of mouse brains was double-stained with COX-2 (green) and Aβ (red) (C) or Iba1 (red) (D) antibody before observation using confocal microscopy. The data are represented as the means ± S.E. $^{**}p < 0.01$ with respect to WT mice

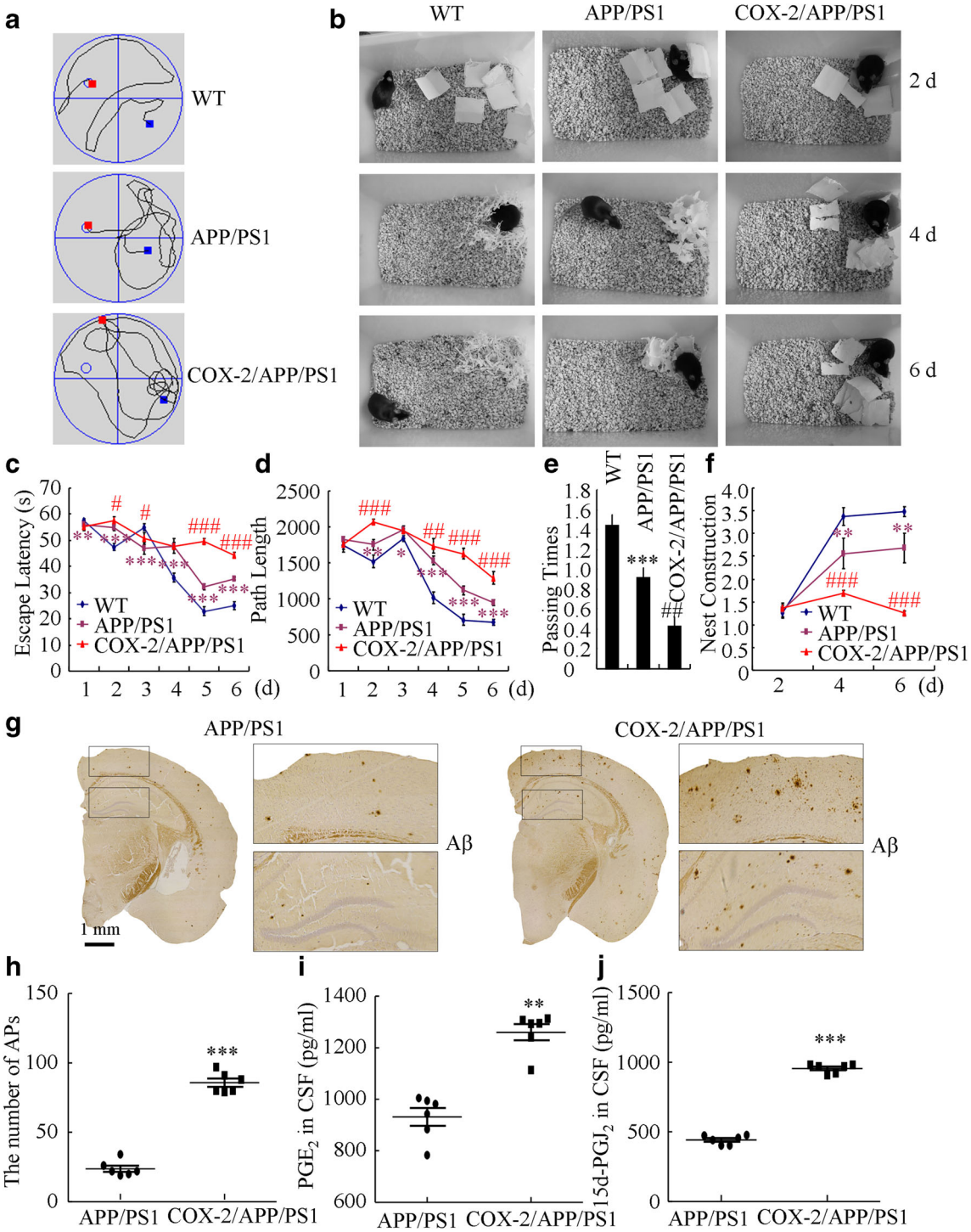

Fig. 2 COX-2 elevation is critical for elevating the production of PGE_2 and 15d-PGJ_2 as well as for the deposition of Aβ, which accelerates the cognitive decline of APP/PS1 mice. COX-2 mice were bred with APP/PS1 mice to obtain the COX-2/APP/PS1 mice, and genotyping was performed at the age of 1 month. Performance on the (A) Morris water maze test and (B) nest construction was analyzed. (C, D) Escape latency and path length were determined in the first 6 days of hidden platform tests. (E) The probe trials were conducted on day 7. (F) Nest construction was quantified in WT, APP/PS1, and COX-2/APP/PS1 mice. The nesting scores were analyzed by the methods described in the "Experimental Procedures." (G, H) The right halves of brains were stained with an Aβ antibody before analysis by microscopy. (I, J) The production of PGE_2 and 15d-PGJ_2 in the CSF of APP/PS1 and COX-2/APP/PS1 mice was determined by PGE_2 and 15d-PGJ_2 ELISA kits. $^{*}p < 0.05$; $^{**}p < 0.01$; $^{***}p < 0.001$ compared with the WT group. $\#p < 0.05$; $\#\#p < 0.01$; $\#\#\#p < 0.001$ compared with APP/PS1 mice ($n = 6$)

COX-2 Expression Plays Pivotal Roles in the Deposition of Aβ in APP/PS1 Mice

Our observation that COX-2 overexpression induced cognitive impairment in 6-month-old APP/PS1 mice raised the question of whether pathological changes appear in a COX-2-dependent manner. As expected, COX-2 expression in APP/PS1 mice appeared with the early onset of AP burden at 6 months old (Fig. 2G, H). These observations clearly demonstrated that COX-2 overexpression has the ability to impair the learning ability by accelerating the deposition of Aβ in APs.

As an enzyme involved in the synthesis of PGH_2, COX-2 could not directly induce Aβ deposition in APs. COX-2 usually enhances $Aβ_{1–42}$ production and deposition via elevating the levels of PGE_2 [46, 47] and PGD_2 [and its dehydration end product 15d-PGJ_2] [48–50]. To investigate the roles of PGE_2 and 15d-PGJ_2 in AD development, we first determined their concentrations in the CSF of APP/PS1 and COX-2/APP/PS1 mice. The production of PGE_2 and 15d-PGJ_2 was markedly induced in 6-month-old COX-2/APP/PS1 mice compared with that in 6-month-old APP/PS1 mice (Fig. 2I, J). These observations clearly indicated that COX-2 expression accelerates the production of PGE_2 and 15d-PGJ_2 during the course of AD development and progression.

The Expression of TNF-α and PS1/2 Is Progressively Upregulated with the Development of AD

Because COX-2 and its derived PGs could not exert their effects in a vacuum to accelerate the deposition of Aβ, we were prompted to identify the molecules that are involved in this process. In light of possible contributions of TNF-α to Aβ deposition, we first determined the expression of TNF-α in the brains of APP/PS1 mice. The protein expression of TNF-α was significantly upregulated in the brains of APP/PS1 mice at different ages (Fig. 3A). These data strongly suggest an involvement of TNF-α in the pathogenesis of AD; however, it might not be a direct trigger for the origination of Aβ deposition because Aβ is the cleavage product of APP by β- or γ-secretases. Indeed, prior research suggests that TNF-α regulates APP processing and Aβ deposition by activating PS1 and PS2 in neurons [32, 33]. To this end, we further determined the expression of PS1 and PS2 in APP/PS1 mice at different stages. The mRNA and protein expression levels of PS1 and PS2 were elevated with the development of AD (Fig. 3B). To further determine the morphological changes of PS1 and PS2, immunohistochemistry experiments were carried out in APP/PS1 and COX-2/APP/PS1 mice. PS1 and PS2 seemed to be localized in the neurons of COX-2/APP/PS1 (Fig. 3C). To further determine the localization of PS1/2, double-staining for PS1/2 and NeuN in the brains of APP/PS1 Tg mice was carried out in immunofluorescence experiments, revealing that PS1/2 colocalized with neurons (Fig. 3D). These findings clearly indicated the potential involvement of TNF-α and PS1/2 in mediating COX-2-exacerbated AD progression.

NS398 Inhibits the Synthesis of TNF-α and PS1/2 Via mPGES-1 and PGE_2 but not L-PGDS and 15d-PGJ_2 in COX-2/APP/PS1 Mice

To further elucidate the roles of COX-2 in regulating the expression of TNF-α and PS1/2, we investigated the potential contributions of PGE_2 and 15d-PGJ_2 to COX-2-dependent TNF-α and PS1/2 synthesis in COX-2/APP/PS1 mice, revealing that mPGES-1 expression and the production of PGE_2 were markedly induced in 6-month-old COX-2/APP/PS1 mice (Fig. 4A, D, E). Intracerebroventricular injection of a COX-2-specific inhibitor, NS398 (1 μg/5 μl), into 6-month-old COX-2/APP/PS1 mice clearly inhibited the expression of mPGES-1 and the production of PGE_2 without affecting the expression of L-PGDS and the production of 15d-PGJ_2 (Fig. 4A, B, D, E). The regulation of TNF-α and PS1/2 was similar to that of mPGES-1 and PGE_2 in 6-month-old COX-2-overexpressing APP/PS1 mice (Fig. 4C–E). With the injection (i.c.v.) of NS398 (1 μg/5 μl) to 6-month-old COX-2/APP/PS1 mice, the upregulation of TNF-α and PS1/2 was attenuated (Fig. 4C–E). These data implied the possible contributions of mPGES-1 and PGE_2 in regulating the expression of TNF-α and PS1/2 at the early stage of AD.

PGE_2 Facilitates the Deposition of Aβ in APs, Which Is Critical for the Cognitive Decline of APP/PS1 Mice

In view of the critical effects of PGE_2 on the expression of TNF-α and PS1/2, we further determined their functions in Aβ aggregation. As a first step, 3-month-old APP/PS1 mice were intranasally administered PGE_2 (2 μg/20 μl/day) for 3 months before their brains were collected. PGE_2 treatment clearly increased the number of APs in the brain cerebral cortex and hippocampus (Fig. 5A). In view of these observations, we further determined its effects on the learning ability of APP/PS1 Tg mice, revealing that PGE_2 treatment for 3 months accelerated the cognitive decline of APP/PS1 mice at the age of 6 months (Fig. 5B–E).

Low Concentrations of 15d-PGJ_2 Stimulated the Expression of TNF-α and PS1/2, Whereas High Concentrations of 15d-PGJ_2 Depressed the Expression of TNF-α and PS1/2

In view of the possible roles of PGE_2 and 15d-PGJ_2 in AD progression [27, 28], we next aimed to determine the potential contributions of COX-2-derived 15d-PGJ_2 to Aβ deposition in the brains of APP/PS1 mice. For this purpose, we first

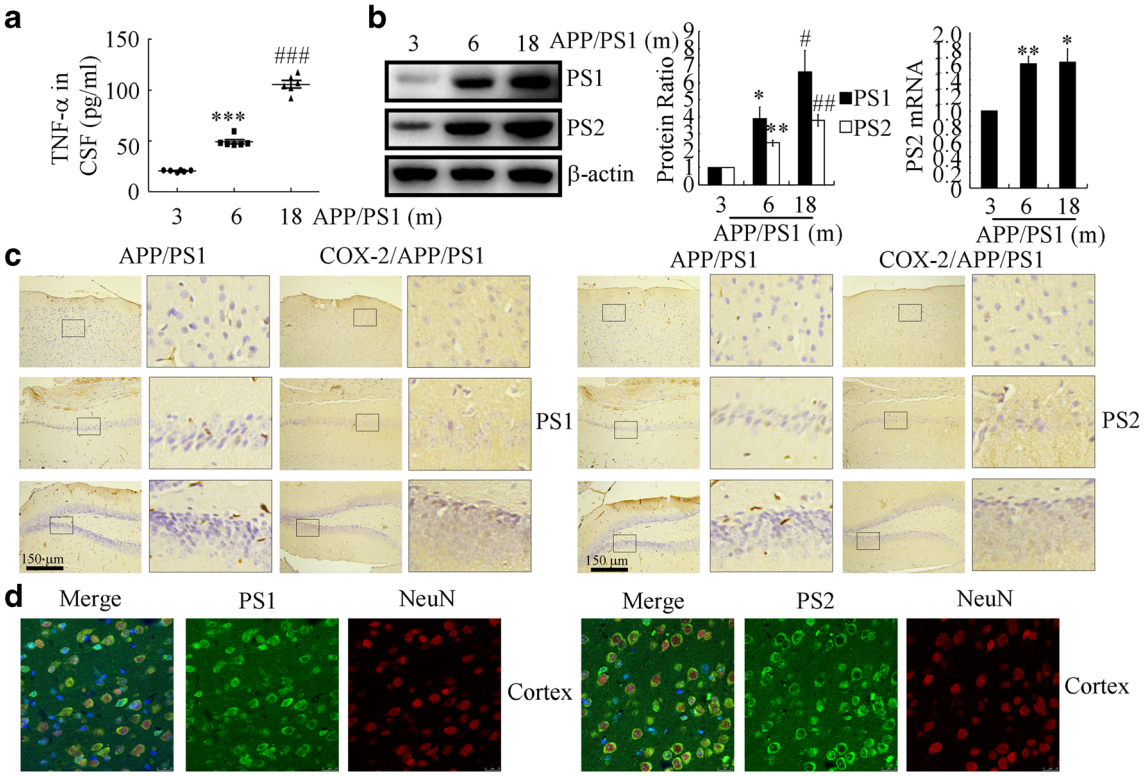

Fig. 3 The expression of TNF-α and PS1/2 is progressively upregulated during the course of AD development. (A) The production of TNF-α in the CSF of APP/PS1 mice was determined by ELISA. (B) The PS1 and PS2 mRNA and protein levels were determined by Western blots and qRT-PCR. (C) The immunoreactivities of PS1 and PS2 in the cerebral cortex and hippocampus of 6-month-old APP/PS1 and COX-2/APP/PS1 mice were determined by immunohistochemistry using an anti-PS1 or PS2 antibody, respectively. (D) The cerebral cortex and hippocampus of mouse brains were double-stained with PS1/2 (red) and NeuN (green) antibody before observation using confocal microscopy. The data are represented as the means ± S.E. $*p < 0.05$; $**p < 0.01$; $***p < 0.001$ with respect to the 3-month-old APP/PS1 mice. $\#p < 0.05$; $\#\#p < 0.01$; $\#\#\#p < 0.001$ compared with 6-month-old APP/PS1 mice ($n = 6$)

treated the N2a cells with the indicated concentration of 15d-PGJ_2 for 48 h, revealing that a low concentration of 15d-PGJ_2 markedly stimulated the protein expression of TNF-α and PS1/2 (Fig. 6A, B). The protein levels of TNF-α and PS1/2

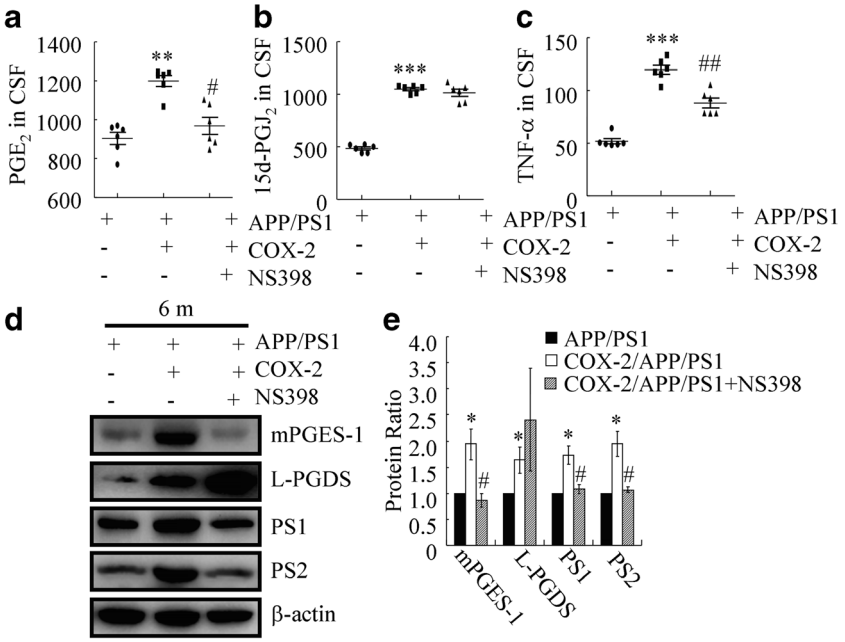

Fig. 4 NS398 suppresses the synthesis of TNF-α and PS1/2 via PGE_2. NS398 (1 μg/5 μl) was injected (i.c.v.) into the ventricles of 6-month-old COX-2/APP/PS1 mice for 24 h. The brains and CSF were then collected after anesthetization. (A–C) The formation of PGE_2 and 15d-PGJ_2 and the secretion of TNF-α were assessed using PGE_2, 15d-PGJ_2, and TNF-α enzyme immunoassay kits, respectively. (D, E) Protein expression of mPGES-1, L-PGDS, PS1, and PS2 was determined by Western blots. β-Actin served as an internal control. $**p < 0.01$; $***p < 0.001$ with respect to the APP/PS1 group. $\#p < 0.05$; $\#\#p < 0.01$ compared with COX-2/APP/PS1 mice ($n = 6$)

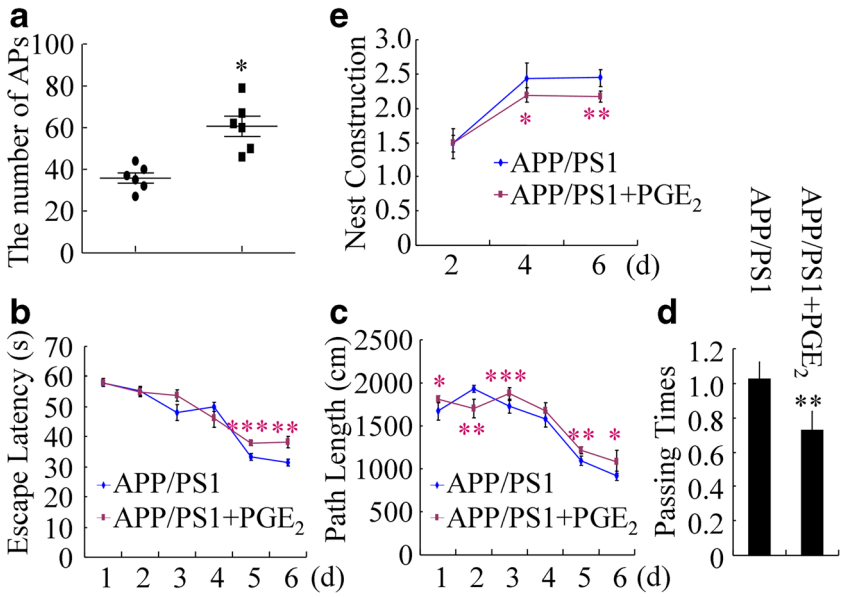

Fig. 5 PGE_2 accelerates the aggregation of Aβ and the cognitive decline of APP/PS1 mice. APP/PS1 mice at the age of 3 months were intranasally treated with PGE_2 (2 μg/20 μl/day) for 3 months. (A) The brains were stained with an Aβ antibody before analysis by microscopy. (B–E) The learning abilities of different groups of mice were assessed by the Morris water maze test or nest construction assay. $*p < 0.05$; $**p < 0.01$; $***p < 0.001$ with respect to the APP/PS1 group ($n = 6$)

reached a maximum plateau when the concentration of 15d-PGJ_2 was increased to 20 nM and then returned toward the basal levels (Fig. 6A, B). Notably, the expression of TNF-α and PS1/2 was significantly suppressed when N2a cells were treated with 500 nM 15d-PGJ_2 for 24 h (Fig. 6A, B). To further confirm these *in vitro* results, 6-month-old APP/PS1 mice were intranasally administered different concentrations of 15d-PGJ_2 for 24 h. 15d-PGJ_2 treatment at 10 ng/20 μl markedly increased the protein expression of TNF-α and PS1/2 in APP/PS1 mice (Fig. 6C, D). In contrast, a high concentration of 15d-PGJ_2 (1000 ng/20 μl) obviously suppressed the expression of TNF-α and PS1/2 in APP/PS1 mice (Fig. 6C, D). Based on these *in vitro* and *in vivo* experiments, our data demonstrated that a low concentration of 15d-PGJ_2 stimulated the expression of TNF-α and PS1/2, whereas a high concentration of 15d-PGJ_2 depressed the expression of TNF-α and PS1/2.

Either Low or High Concentrations of 15d-PGJ_2 Impaired the Learning Ability of APP/PS1 Mice

After observation of the antagonistic effects of low and high concentrations of 15d-PGJ_2 on the expression of TNF-α and PS1/2, we continued to assess the effects of different concentrations of 15d-PGJ_2 on the deposition of Aβ and the learning ability of APP/PS1 mice. For this purpose, 3-month-old APP/PS1 mice were intranasally administered 15d-PGJ_2 (20 or 1000 ng/20 μl/day) for 3 months before their brains were

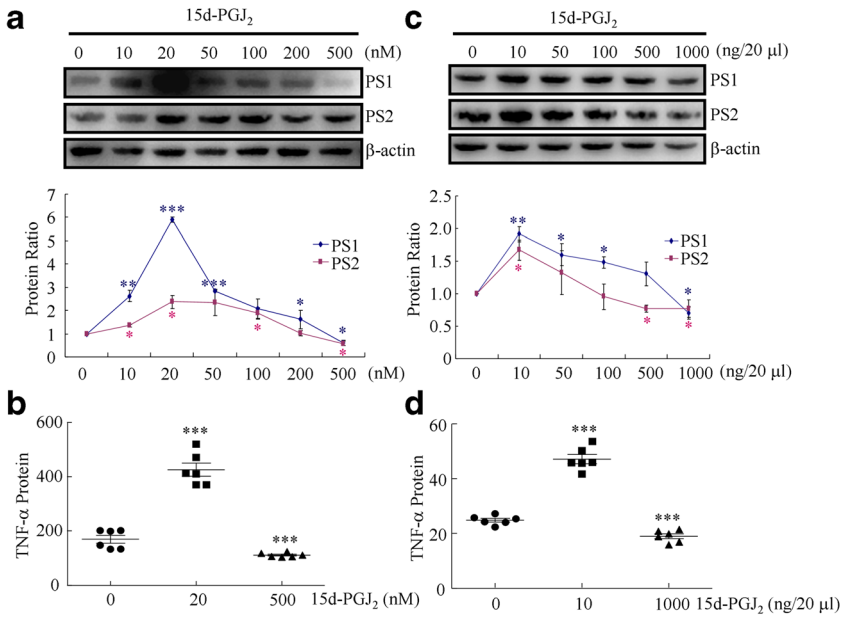

Fig. 6 The expression of TNF-α and PS1/2 is stimulated by low concentration of 15d-PGJ_2 but inhibited by high concentration of 15d-PGJ_2. (A, B) N2a cells were treated with different concentrations of 15d-PGJ_2 for 24 h. (C, D) The APP/PS1 mice were intranasally treated with the indicated concentration of 15d-PGJ_2 for 24 h ($n = 6$). (A, C) The PS1 and PS2 protein levels were determined by Western blots. β-Actin served as an internal control. (B, D) The production of TNF-α in the CSF of APP/PS1 mice was determined by ELISA. The data presented as the means ± S.E. $*p < 0.05$; $**p < 0.01$; $***p < 0.001$ with respect to the vehicle-treated controls

collected. Low or high concentrations of 15d-PGJ_2 treatment showed antagonistic effects on the deposition of Aβ to APs in the brains of APP/PS1 mice (Fig. 7A). In view of these observations, we further determined its effects on the learning ability of APP/PS1 Tg mice. Surprisingly, either low or high concentrations of 15d-PGJ_2 treatment accelerated the cognitive decline of APP/PS1 mice at the age of 6 months (Fig. 7B–E).

High Concentration of 15d-PGJ_2 Induced the Apoptosis of Neurons, Which Underlies the Cognitive Decline of APP/PS1 Mice

Because a high concentration of 15d-PGJ_2 showed the inhibitory effects on Aβ aggregation but did not improve the learning ability of APP/PS1 mice, we were prompted to elucidate the inherent mechanisms. To this end, experiments were carried out to determine the effects of different concentrations of 15d-PGJ_2 on the neuronal apoptosis. The treatment of N2a cells with a high concentration of 15d-PGJ_2 (500 nM) for 24 h obviously induced the expression of Bax and the production of cleaved caspase-3 and DFF45 (Fig. 8A, B). In addition, intranasal administration of APP/PS1 mice with high concentrations of 15d-PGJ_2 (1000 ng/20 μl) for 24 h similarly increased the expression of Bax and the production of cleaved caspase-3 and DFF45 (Fig. 8C, D). Based on these observations, it is clear that a high concentration of 15d-PGJ_2 impairs the learning ability of APP/PS1 mice by inducing neuronal apoptosis.

Taken together, these results clearly show that overexpression of COX-2 in APP/PS1 mice has the ability to increase the aggregation of $A\beta_{1-42}$ via an mPGES-1- and PGE_2-dependent mechanism, and this phenomenon impairs the learning ability of APP/PS1 mice at the early stage of AD. In addition, 15d-PGJ_2 accumulation at the late stage of AD is able to induce the cognitive decline of APP/PS1 mice via apoptotic mechanisms.

Discussion

AD is pathologically characterized by the production and aggregation of Aβ in the brain. Although certain phenomena by which COX-2 [14, 51] and TNF-α [27, 28, 32] regulate the pathogenesis of AD have been proposed, the relationship among COX-2, TNF-α, and Aβ [52] is still unclear. To this end, the purpose of the current study was to decipher the mechanisms of COX-2 in regulating Aβ deposition via TNF-α, which potentially contributes to the cognitive decline of AD patients. The major findings of this study are as follows: 1) elevated expression of COX-2 in AD experimental models upregulates the expression of mPGES-1, PGE_2, L-PGDS, and 15d-PGJ_2 during the course of AD development and progression; 2) PGE_2 is responsible for Aβ deposition via a TNF-α-dependent PS1/2-activating mechanisms at the early stage of AD; and 3) despite that highly induced 15d-PGJ_2 at the late stage of AD inhibits the aggregation of Aβ via inhibiting the expression of TNF-α and PS1/2, it still impairs the learning ability of APP/PS1 mice via activating neuronal apoptosis.

As the key enzyme responsible for inflammation, COX-2 is tightly regulated under physiological conditions. In response to the onset of AD, COX-2 was found to be activated at the early stage of the disease, and its activity was decreased during later stages of the disease accompanied by the production of PGE_2 [53]. In line with prior reports [53], our data demonstrated that COX-2 expression was markedly upregulated at the early stage of the disease in the brains of AD patients, and its expression was reduced at the late stage of the disease accompanied by a disruption of neuronal cells. In APP/PS1 transgenic mice, the expression of COX-2 is somewhat complicated. In 3- and 6-month-old APP/PS1 transgenic mice, COX-2 expression was upregulated, whereas COX-2 in 18-month-old mice appeared to aggregate with the APs.

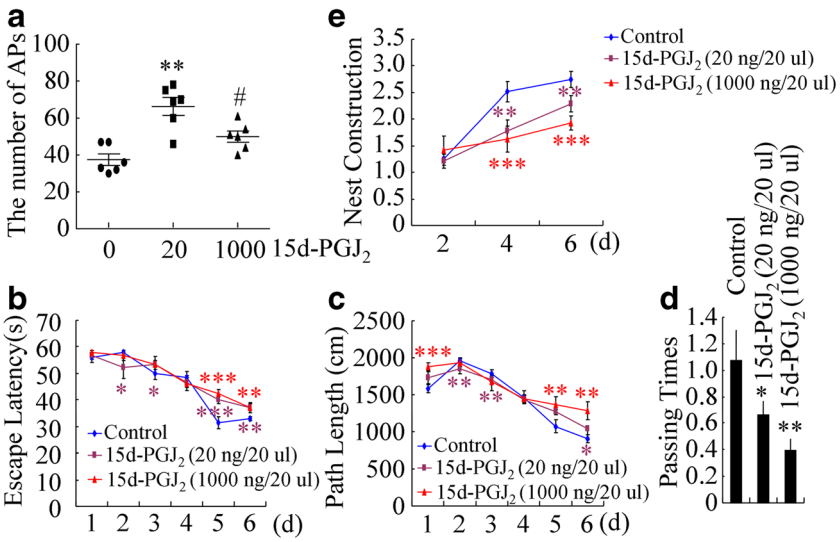

Fig. 7 Either low or high concentrations of 15d-PGJ_2 impair the learning ability of APP/PS1 mice. APP/PS1 mice at the age of 3 months were intranasally treated with 15d-PGJ_2 at a concentration of 20 ng/20 μl/day or 1000 ng/20 μl/day for 3 months. The brains were collected after anesthetization. (A) The brains were then stained with an Aβ antibody before analysis by microscopy. (B–E) The learning abilities of different groups of mice were assessed by the Morris water maze test or nest construction assay. $^*p < 0.05$; $^{**}p < 0.01$; $^{***}p < 0.001$ with respect to the APP/PS1 group ($n = 6$)

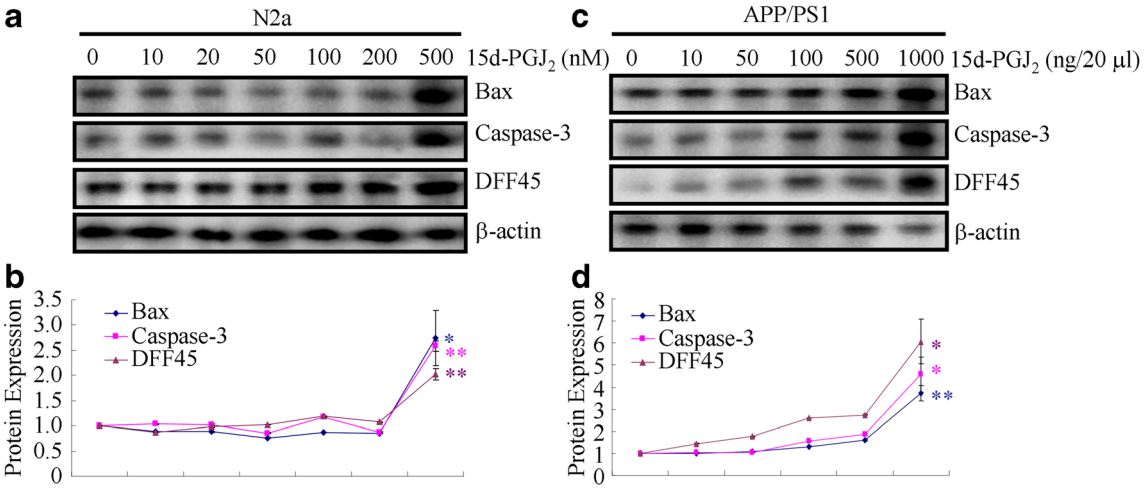

Fig. 8 High concentrations of 15d-PGJ_2 impairs the learning ability of APP/PS1 mice via apoptotic mechanisms. (A, B) N2a cells were treated with the indicated concentration of 15d-PGJ_2 for 24 h. (C, D) The APP/PS1 mice were intranasally treated with the indicated concentration of 15d-PGJ_2 for 24 h ($n = 6$). The protein levels of Bax and cleaved caspase-3 and DFF45 were determined by Western blots. β-Actin served as an internal control. The data are presented as the means ± S.E. $^{*}p < 0.05$; $^{**}p < 0.01$; $^{***}p < 0.001$ with respect to the vehicle-treated controls

Although we could not directly compare the late-stage AD patients with 18-month-old APP/PS1 transgenic mice, our observations indicate that COX-2 might be able to bind Aβ. In line with our hypothesis, Nagano et al. [45] verified that COX-2 is able to cross-link with Aβ, generating Aβ-COX-2 hetero-oligomers, which are increased in AD. This observation concretely supports our data showing that COX-2 colocalized and bound to Aβ in 18-month-old mice.

Given the interaction between COX-2 and $Aβ_{1–42}$, the interest in the COX-2 investigation was prompted by the application of NSAIDs [54]. For example, COX-2 inhibition by NSAIDs has been shown to have protective effects against AD progression [14]. In addition, blockade of COX-2 by flavocoxid was able to counteract the progression of AD [55]. However, animal experiments might not provide useful guidance for clinical trials because PGs play different roles in AD development [56]. To this end, our data revealed that PGE_2 and PGD_2 are elevated in COX-2-overexpressing APP/PS1 mice. To study the roles of PGE_2 and PGD_2 in AD, we first treated the COX-2/APP/PS1 mice with the COX-2 specific inhibitor, NS398. The results demonstrated that NS398 treatment significantly blocked the effects of COX-2 on stimulating the expression of mPGES-1 and PS1/2 as well as the production of PGE_2 and TNF-α, without affecting the expression of L-PGDS or the production of the dehydrated of PGD_2 product, 15d-PGJ_2 (Fig. 4). In line with our observation, Matsumoto et al. [57] reported that COX-2 induction markedly increases the conversion to PGE_2, which parallels the mPGES-1 induction in macrophages. More closely, Vazquez-Tello et al. [58] further found colocalization between COX-2 and mPGES-1 in the brains of Wistar rats. In line with these observations, NS398 was found to inhibit mPGES-1 expression and PGE_2 production in human A549 cells and gastric fibroblasts [59, 60]. Along these lines, PGE_2 was indicated to be critical for the pathogenesis of AD. As expected, our data further showed that PGE_2 treatment clearly accelerated the deposition of Aβ and the cognitive decline of APP/PS1 mice via TNF-α-dependent PS1/2-activating mechanisms (Fig. 5). In agreement with our observations, Renz et al. [61] reported that PGE_2 stimulated the production of TNF-α in a cGMP-dependent manner in rat macrophages. As an important proinflammatory cytokine, highly induced TNF-α was reported to accelerate the progression of AD [62]. This finding is substantiated by prior observations showing that TNF-α upregulates APP processing and Aβ deposition in human rhabdomyosarcoma [25] and neuroblastoma cells [26]. Additionally, our data are further supported by reports demonstrating that anti-TNF-α or inhibition of TNF-α signaling reduces the formation of APs in the brains of APP/PS1 transgenic mice [27, 28]. Indeed, Satoh and Kuo et al. [32, 33] have suggested that TNF-α regulates APP processing and Aβ deposition by activating PS1 and PS2 in neuronal cells. These *in vitro* and *in vivo* data are clearly in agreement with our data suggesting that PGE_2 regulates the formation of Aβ via TNF-α-dependent PS1/2-activating mechanisms in neuronal cells.

In contrast to mPGES-1 and PGE_2, NS398 is not able to suppress the expression of L-PGDS or the production of 15d-PGJ_2 (Fig. 4D, E). However, COX-2 overexpression clearly induced the expression of L-PGDS in 6-month-old COX-2/APP/PS1 mice (Fig. 4D, E). Because PGE_2 accelerated the deposition of Aβ to APs, we suspected that the upregulation of L-PGDS was caused by APs. Indeed, the formation of APs has been suggested to upregulate the expression of H-PGDS and the DP1 receptor in the microglia and astrocytes of AD patients and Tg2576 mice [63]. Therefore, it is possible that the upregulation of L-PGDS and the induction of 15d-PGJ_2

are caused by the deposition of Aβ in a PGE_2-dependent manner.

Compared to those of PGE_2, the biological functions of 15d-PGJ_2 seemed to be slightly complicated. At low concentrations, 15d-PGJ_2 exerted a stimulatory effect on neuroinflammation (Fig. 6). In addition, a low concentration of 15d-PGJ_2 increased the number of APs in the brains of APP/PS1 mice (Fig. 7A). In concert with our observations, PGD_2 treatment increased the production of $A\beta_{1–42}$ in primary cultured mouse neuronal cells [48]. Similarly, 15d-PGJ_2 treatment induced fibrillar Aβ in rat cortical neurons [49, 50]. More interestingly, Koh et al. [64] suggested that 15d-PGJ_2 acted as a neuroprotectant or neurotoxicant depending on its concentration. High concentration of 15d-PGJ_2 likely showed suppressive effects on the expression of TNF-α and PS1/2 *in vitro* and *in vivo* (Fig. 6). Although there is no direct evidence supporting our data, PGD_2 and 15d-PGJ_2 have shown suppressive effects on the expression of TNF-α. For example, anti-inflammatory effects of PGD_2 have now been recognized in leukocytes and other cells, especially after identification of its dehydrated metabolite, 15d-PGJ_2 [65]. 15d-PGJ_2 appeared to be more efficient in reducing the expression of TNF-α in THP-1 monocytes [66]. The observation that a high concentration of 15d-PGJ_2 inhibited the deposition of Aβ raised the question of whether high concentration of 15d-PGJ_2 can improve the cognitive decline of APP/PS1 mice. Unfortunately, a high concentration of 15d-PGJ_2 further impaired the learning ability of APP/PS1 mice (Fig. 7B–E). To explain this phenomenon, we further explored the effects of 15d-PGJ_2 on the neuronal apoptosis. As expected, highly accumulated 15d-PGJ_2 showed the ability to induce the neuronal apoptosis by inducing the expression of Bax and the production of cleaved caspase-3 and DFF45, which resulted in the cognitive decline of AD (Fig. 8). In line with our data, 15d-PGJ_2 has shown its effects on inducing neuronal cell apoptosis [67].

Taken together, these results show that COX-2 expression is upregulated at the early stage of AD, and this phenomenon is responsible for elevating the expression of mPGES-1 and PGE_2 in 6-month-old APP/PS1 mice. PGE_2 accumulation regulates Aβ deposition by modulating TNF-α-dependent PS1/2 activity. L-PGDS and 15d-PGJ_2 are induced by Aβ fibrils at the late stage of AD and, thus, play dual roles in the production and deposition of Aβ. On the one hand, a low concentration of 15d-PGJ_2 has the ability to induce the production and deposition of Aβ via stimulating the expression of TNF-α and PS1/2. On the other hand, a high concentration of 15d-PGJ_2 can suppress the formation of Aβ fibrils, which seems to be beneficial for treating AD. However, a high concentration of 15d-PGJ_2 induces the neuronal death, which further impairs the learning ability of APP/PS1 mice.

Acknowledgments This work was supported in part or in whole by the Natural Science Foundation of China (81870840, 31571064, 81771167, and 81500934) and the Fundamental Research Foundation of Northeastern University, China (N172008008 and N172004005).

Required Author Forms Disclosure forms provided by the authors are available with the online version of this article.

Compliance with Ethical Standards All animals were handled according to the Guide for the Care and Use of Medical Laboratory Animals (Ministry of Health, People's Republic of China, 1998), and all experimental protocols were approved by the Laboratory Ethics Committees of China Medical University and the College of Life and Health Sciences of Northeastern University.

Conflict of Interest The authors declare that they have no conflict of interest.

References

1. Melnikova T, Savonenko A, Wang Q, et al. Cycloxygenase-2 activity promotes cognitive deficits but not increased amyloid burden in a model of Alzheimer's disease in a sex-dimorphic pattern. Neuroscience 2006;141:1149–1162.
2. Xiang Z, Ho L, Valdellon J, et al. Cyclooxygenase (COX)-2 and cell cycle activity in a transgenic mouse model of Alzheimer's disease neuropathology. Neurobiol Aging 2002;23:327–334.
3. Xiang Z, Ho L, Yemul S, et al. Cyclooxygenase-2 promotes amyloid plaque deposition in a mouse model of Alzheimer's disease neuropathology. Gene Expr 2002;10:271–278.
4. Kadoyama K, Takahashi Y, Higashida H, Tanabe T, Yoshimoto T: Cyclooxygenase-2 stimulates production of amyloid beta-peptide in neuroblastoma x glioma hybrid NG108-15 cells. Biochem Biophys Res Commun 2001;281:483–490.
5. Kukar T, Prescott S, Eriksen JL, et al. Chronic administration of R-flurbiprofen attenuates learning impairments in transgenic amyloid precursor protein mice. BMC Neurosci 2007;8:54.
6. Jantzen PT, Connor KE, DiCarlo G, et al. Microglial activation and beta-amyloid deposit reduction caused by a nitric oxide-releasing nonsteroidal anti-inflammatory drug in amyloid precursor protein plus presenilin-1 transgenic mice. J Neurosci 2002;22:2246–2254.
7. Akitake Y, Nakatani Y, Kamei D, et al. Microsomal prostaglandin e synthase-1 is induced in Alzheimer's disease and its deletion mitigates Alzheimer's disease-like pathology in a mouse model. J Neurosci Res 2013;91:909–919.
8. Hein AM, Stutzman DL, Bland ST, et al. Prostaglandins are necessary and sufficient to induce contextual fear learning impairments after interleukin-1 beta injections into the dorsal hippocampus. Neuroscience 2007;150:754–763.
9. Matsumoto Y, Yamaguchi T, Watanabe S, Yamamoto T: Involvement of arachidonic acid cascade in working memory impairment induced by interleukin-1 beta. Neuropharmacology 2004;46:1195–1200.
10. Hoshino T, Namba T, Takehara M, et al. Improvement of cognitive function in Alzheimer's disease model mice by genetic and pharmacological inhibition of the EP(4) receptor. J Neurochem 2012;120:795–805.
11. Shi J, Wang Q, Johansson JU, et al. Inflammatory prostaglandin E2 signaling in a mouse model of Alzheimer disease. Ann Neurol 2012;72:788–798.
12. Nishida N, Nagata N, Toda H, et al. Association of lipocalin-type prostaglandin D synthase with disproportionately enlarged subarachnoid-space in idiopathic normal pressure hydrocephalus. Fluids Barriers CNS 2014;11:9.

13. Kanekiyo T, Ban T, Aritake K, et al. Lipocalin-type prostaglandin D synthase/beta-trace is a major amyloid beta-chaperone in human cerebrospinal fluid. Proc Natl Acad Sci U S A 2007;104:6412–6417.
14. Szekely CA, Thorne JE, Zandi PP, et al. Nonsteroidal anti-inflammatory drugs for the prevention of Alzheimer's disease: a systematic review. Neuroepidemiology 2004;23:159–169.
15. Heneka MT, Sastre M, Dumitrescu-Ozimek L, et al. Acute treatment with the PPARgamma agonist pioglitazone and ibuprofen reduces glial inflammation and Abeta1-42 levels in APPV717I transgenic mice. Brain 2005;128:1442–1453.
16. Lim GP, Yang F, Chu T, et al. Ibuprofen suppresses plaque pathology and inflammation in a mouse model for Alzheimer's disease. J Neurosci 2000;20:5709–5714.
17. McKee AC, Carreras I, Hossain L, et al. Ibuprofen reduces Abeta, hyperphosphorylated tau and memory deficits in Alzheimer mice. Brain Res 2008;1207:225–236.
18. Morihara T, Teter B, Yang F, et al. Ibuprofen suppresses interleukin-1beta induction of pro-amyloidogenic alpha1-antichymotrypsin to ameliorate beta-amyloid (Abeta) pathology in Alzheimer's models. Neuropsychopharmacology 2005;30:1111–1120.
19. Yan Q, Zhang J, Liu H, et al. Anti-inflammatory drug therapy alters beta-amyloid processing and deposition in an animal model of Alzheimer's disease. J Neurosci 2003;23:7504–7509.
20. Coma M, Sereno L, Da Rocha-Souto B, et al. Triflusal reduces dense-core plaque load, associated axonal alterations and inflammatory changes, and rescues cognition in a transgenic mouse model of Alzheimer's disease. Neurobiol Dis 2010;38:482–491.
21. Lee EO, Shin YJ, Chong YH: Mechanisms involved in prostaglandin E2-mediated neuroprotection against TNF-alpha: possible involvement of multiple signal transduction and beta-catenin/T-cell factor. J Neuroimmunol 2004;155:21–31.
22. Maesaka JK, Sodam B, Palaia T, et al. Prostaglandin D2 synthase: apoptotic factor in Alzheimer plasma, inducer of reactive oxygen species, inflammatory cytokines and dialysis dementia. J Nephropathol 2013;2:166–180.
23. Drew PD, Chavis JA: The cyclopentone prostaglandin 15-deoxy-delta(12,14) prostaglandin J2 represses nitric oxide, TNF-alpha, and IL-12 production by microglial cells. J Neuroimmunol 2001;115:28–35.
24. Giri S, Rattan R, Singh AK, Singh I: The 15-deoxy-delta12,14-prostaglandin J2 inhibits the inflammatory response in primary rat astrocytes via down-regulating multiple steps in phosphatidylinositol 3-kinase-Akt-NF-kappaB-p300 pathway independent of peroxisome proliferator-activated receptor gamma. J Immunol 2004;173:5196–5208.
25. Keller CW, Schmitz M, Munz C, Lunemann JD, Schmidt J: TNF-alpha upregulates macroautophagic processing of APP/beta-amyloid in a human rhabdomyosarcoma cell line. J Neurol Sci 2013;325:103–107.
26. Blasko I, Marx F, Steiner E, Hartmann T, Grubeck-Loebenstein B: TNFalpha plus IFNgamma induce the production of Alzheimer beta-amyloid peptides and decrease the secretion of APPs. FASEB J 1999;13:63–68.
27. McAlpine FE, Lee JK, Harms AS, et al. Inhibition of soluble TNF signaling in a mouse model of Alzheimer's disease prevents pre-plaque amyloid-associated neuropathology. Neurobiol Dis 2009;34:163–177.
28. Shi JQ, Shen W, Chen J, et al. Anti-TNF-alpha reduces amyloid plaques and tau phosphorylation and induces CD11c-positive dendritic-like cell in the APP/PS1 transgenic mouse brains. Brain Res 2011;1368:239–247.
29. Hong HS, Hwang EM, Sim HJ, et al. Interferon gamma stimulates beta-secretase expression and sAPPbeta production in astrocytes. Biochem Biophys Res Commun 2003;307:922–927.
30. Satoh J, Kuroda Y: Amyloid precursor protein beta-secretase (BACE) mRNA expression in human neural cell lines following induction of neuronal differentiation and exposure to cytokines and growth factors. Neuropathology 2000;20:289–296.
31. Yamamoto M, Kiyota T, Horiba M, et al. Interferon-gamma and tumor necrosis factor-alpha regulate amyloid-beta plaque deposition and beta-secretase expression in Swedish mutant APP transgenic mice. Am J Pathol 2007;170:680–692.
32. Kuo LH, Hu MK, Hsu WM, et al. Tumor necrosis factor-alpha-elicited stimulation of gamma-secretase is mediated by c-Jun N-terminal kinase-dependent phosphorylation of presenilin and nicastrin. Mol Biol Cell 2008;19:4201–4212.
33. Satoh J, Kuroda Y: Constitutive and cytokine-regulated expression of presenilin-1 and presenilin-2 genes in human neural cell lines. Neuropathol Appl Neurobiol 1999;25:492–503.
34. Bernardo A, Levi G, Minghetti L: Role of the peroxisome proliferator-activated receptor-gamma (PPAR-gamma) and its natural ligand 15-deoxy-delta12, 14-prostaglandin J2 in the regulation of microglial functions. Eur J Neurosci 2000;12:2215–2223.
35. Kyrkanides S, Moore AH, Olschowka JA, et al. Cyclooxygenase-2 modulates brain inflammation-related gene expression in central nervous system radiation injury. Brain Res Mol Brain Res 2002;104:159–169.
36. Petrova TV, Akama KT, Van Eldik LJ: Cyclopentenone prostaglandins suppress activation of microglia: down-regulation of inducible nitric-oxide synthase by 15-deoxy-delta12,14-prostaglandin J2. Proc Natl Acad Sci U S A 1999;96:4668–4673.
37. Rohn TT, Wong SM, Cotman CW, Cribbs DH: 15-Deoxy-delta12, 14-prostaglandin J2, a specific ligand for peroxisome proliferator-activated receptor-gamma, induces neuronal apoptosis. Neuroreport 2001;12:839–843.
38. Yu X, Guan PP, Guo JW, et al. By suppressing the expression of anterior pharynx-defective-1alpha and -1beta and inhibiting the aggregation of beta-amyloid protein, magnesium ions inhibit the cognitive decline of amyloid precursor protein/presenilin 1 transgenic mice. FASEB J 2015;29:5044–5058.
39. Wang P, Guan PP, Guo JW, et al. Prostaglandin I2 upregulates the expression of anterior pharynx-defective-1α and -1β in amyloid precursor protein/presenilin1 transgenic mice. Aging Cell 2016; 15, 861–871
40. Wang P, Guan PP, Yu X, Zhang LC, Su YN, Wang ZY: Prostaglandin I2 attenuates prostaglandin E2-stimulated expression of interferon γ in a β-amyloid protein- and NF-κB-dependent mechanism. Scientific Reports 2016; accepted for publication
41. Wang P, Yu X, Guan P-P, et al. Magnesium ion influx reduces neuroinflammation in Aβ precursor protein/presenilin 1 transgenic mice by suppressing the expression of interleukin-1β. Cell Mol Immunol 2015
42. Piermartiri TC, Figueiredo CP, Rial D, et al. Atorvastatin prevents hippocampal cell death, neuroinflammation and oxidative stress following amyloid-beta(1-40) administration in mice: evidence for dissociation between cognitive deficits and neuronal damage. Exp Neurol 2010;226:274–284.
43. Ho L, Purohit D, Haroutunian V, et al. Neuronal cyclooxygenase 2 expression in the hippocampal formation as a function of the clinical progression of Alzheimer disease. Arch Neurol 2001;58:487–492.
44. Montine TJ, Sidell KR, Crews BC, et al. Elevated CSF prostaglandin E2 levels in patients with probable AD. Neurology 1999;53: 1495–1498.
45. Nagano S, Huang X, Moir RD, Payton SM, Tanzi RE, Bush AI: Peroxidase activity of cyclooxygenase-2 (COX-2) cross-links beta-amyloid (Abeta) and generates Abeta-COX-2 hetero-oligomers that are increased in Alzheimer's disease. J Biol Chem 2004;279: 14673–14678.

46. Hoshino T, Nakaya T, Homan T, et al. Involvement of prostaglandin E2 in production of amyloid-beta peptides both in vitro and in vivo. J Biol Chem 2007;282:32676–32688.
47. Hoshino T, Namba T, Takehara M, et al. Prostaglandin E2 stimulates the production of amyloid-beta peptides through internalization of the EP4 receptor. J Biol Chem 2009;284:18493–18502.
48. Bate C, Kempster S, Williams A: Prostaglandin D2 mediates neuronal damage by amyloid-beta or prions which activates microglial cells. Neuropharmacology 2006;50:229–237.
49. Takata K, Kitamura Y, Umeki M, et al. Possible involvement of small oligomers of amyloid-beta peptides in 15-deoxy-delta 12,14 prostaglandin J2-sensitive microglial activation. J Pharmacol Sci 2003;91:330–333.
50. Yamamoto Y, Takase K, Kishino J, et al. Proteomic identification of protein targets for 15-deoxy-delta(12,14)-prostaglandin J2 in neuronal plasma membrane. PLoS One 2011;6:e17552.
51. Teather LA, Packard MG, Bazan NG: Post-training cyclooxygenase-2 (COX-2) inhibition impairs memory consolidation. Learn Mem 2002;9:41–47.
52. Murphy MP, LeVine H, 3rd: Alzheimer's disease and the amyloid-beta peptide. J Alzheimers Dis 2010;19:311–323.
53. Yermakova AV, O'Banion MK: Downregulation of neuronal cyclooxygenase-2 expression in end stage Alzheimer's disease. Neurobiol Aging 2001;22:823–836.
54. Imbimbo BP, Solfrizzi V, Panza F: Are NSAIDs useful to treat Alzheimer's disease or mild cognitive impairment? Front Aging Neurosci 2010;2
55. Bitto A, Giuliani D, Pallio G, et al. Effects of COX1-2/5-LOX blockade in Alzheimer transgenic 3xTg-AD mice. Inflamm Res 2017;66:389–398.
56. Fattahi MJ, Mirshafiey A: Positive and negative effects of prostaglandins in Alzheimer's disease. Psychiatry Clin Neurosci 2014;68: 50–60.
57. Matsumoto H, Naraba H, Murakami M, et al. Concordant induction of prostaglandin E2 synthase with cyclooxygenase-2 leads to preferred production of prostaglandin E2 over thromboxane and prostaglandin D2 in lipopolysaccharide-stimulated rat peritoneal macrophages. Biochem Biophys Res Commun 1997;230:110–114.
58. Vazquez-Tello A, Fan L, Hou X, et al. Intracellular-specific colocalization of prostaglandin E2 synthases and cyclooxygenases in the brain. Am J Physiol Regul Integr Comp Physiol 2004;287: R1155–1163.
59. Shinji Y, Tsukui T, Tatsuguchi A, et al. Induced microsomal PGE synthase-1 is involved in cyclooxygenase-2-dependent PGE2 production in gastric fibroblasts. Am J Physiol Gastrointest Liver Physiol 2005;288:G308–315.
60. Thoren S, Jakobsson PJ: Coordinate up- and down-regulation of glutathione-dependent prostaglandin E synthase and cyclooxygenase-2 in A549 cells. Inhibition by NS-398 and leukotriene C4. Eur J Biochem 2000;267:6428–6434.
61. Renz H, Gong JH, Schmidt A, Nain M, Gemsa D: Release of tumor necrosis factor-alpha from macrophages. Enhancement and suppression are dose-dependently regulated by prostaglandin E2 and cyclic nucleotides. J Immunol 1988;141:2388–2393.
62. Belarbi K, Jopson T, Tweedie D, et al. TNF-alpha protein synthesis inhibitor restores neuronal function and reverses cognitive deficits induced by chronic neuroinflammation. J Neuroinflammation 2012;9:23.
63. Mohri I, Kadoyama K, Kanekiyo T, et al. Hematopoietic prostaglandin D synthase and DP1 receptor are selectively upregulated in microglia and astrocytes within senile plaques from human patients and in a mouse model of Alzheimer disease. J Neuropathol Exp Neurol 2007;66:469–480.
64. Koh SH, Jung B, Song CW, Kim Y, Kim YS, Kim SH: 15-Deoxy-delta12,14-prostaglandin J2, a neuroprotectant or a neurotoxicant? Toxicology 2005;216:232–243.
65. Sandig H, Pease JE, Sabroe I: Contrary prostaglandins: the opposing roles of PGD2 and its metabolites in leukocyte function. J Leukoc Biol 2007;81:372–382.
66. Engdahl R, Monroy MA, Daly JM: 15-Deoxy-delta12,14-prostaglandin J2 (15d-PGJ2) mediates repression of TNF-alpha by decreasing levels of acetylated histone H3 and H4 at its promoter. Biochem Biophys Res Commun 2007;359:88–93.
67. Kondo M, Shibata T, Kumagai T, et al. 15-Deoxy-delta(12,14)-prostaglandin J(2): the endogenous electrophile that induces neuronal apoptosis. Proc Natl Acad Sci U S A 2002;99:7367–7372.